HIGH TEMPERATURE REFLECTANCE SPECTROSCOPY AND DYNAMIC REFLECTANCE SPECTROSCOPY

W. W. WENDLANDT

Thermochemistry Laboratory, Department of Chemistry, University of Houston, Houston, Texas 77004, U.S.A.

ABSTRACT

Two modes of investigation are currently being employed for high temperature reflectance studies. The first is the measurement of the reflectance of a sample at various fixed or isothermal temperatures. Its reflectance spectrum is then scanned over the wavelength region of interest. This mode is called *high temperature reflectance spectroscopy* (HTRS). The second is to record the reflectance change of the sample, at a given wavelength, as a function of temperature. This mode is called *dynamic reflectance spectroscopy* (DRS).

The principles of both of these techniques are discussed along with the instrumentation employed and the application of these techniques to problems of chemical interest. The instrumentation involves the use of a heated sample holder, capable of operation up to 500°C, and a recording spectroreflectometer. The sample holder temperature may be programmed to increase at some fixed rate or maintained at a given temperature.

The techniques of HTRS and DRS are illustrated by their application to the octahedral → tetrahedral transition of $Co(py)_2Cl_2$, the dehydration of cobalt(II) chloride 6-hydrate, the dehydration of $CuSO_4 \cdot 5H_2O$, the thermochromic transition temperature of $M_n[HgI_4]$ complexes, and others.

Also discussed is the new technique of dynamic microreflectance spectroscopy (DMR) and high temperature scanning microreflectance spectroscopy (SMR). The latter techniques are applied to single crystals of various compounds, such as $CuSO_4 \cdot 5H_2O$.

INTRODUCTION

The measurement of the radiation reflected from a mat surface constitutes the area of spectroscopy known as diffuse reflectance spectroscopy. The difference between this technique and transmittance spectroscopy is shown in *Figure 1*. The reflected radiation is expressed as the ratio of I_i/I_r, where I_i is the incident and I_r the reflected radiation. The reflected radiation may be in the ultra-violet, visible, or infra-red regions of the electromagnetic spectrum. From a mat surface, the total reflected radiation, R_T, consists in general of two components: a regular reflectance component (sometimes referred to as surface or mirror reflection), R, and a diffuse reflection component, R_∞[1, 2].

The former component is due to the reflection at the surface of single crystallites while the latter arises from the radiation penetrating into the interior of the solid and re-emerging to the surface after being scattered numerous times.

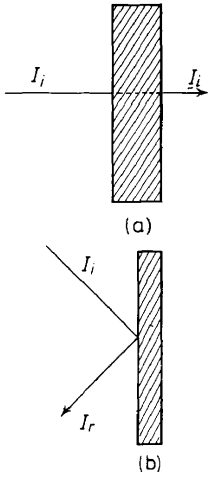

Figure 1. Reflectance and transmittance spectroscopy: (a) Transmittance mode; (b) Reflectance mode.

According to the Kubelka and Munk theory[3], the diffuse reflection component, for 1–3 mm thick layers of a powdered sample (an increase in thickness beyond this point has no effect on the reflectance) at a given wavelength, is equal to

$$R_\infty = \frac{I}{I_0} = \frac{1 - [k/(k + 2s)]^{\frac{1}{2}}}{1 + [k/(k + 2s)]^{\frac{1}{2}}} \tag{1}$$

where I is the reflected radiation, I_0 is the incident radiation, k is the absorption coefficient, and s the scattering coefficient. The absorption coefficient is the same as that given by the familiar Beer–Lambert law, $T = e^{-kd}$. The regular reflection component is governed by one of Fresnel's equations

$$R = \frac{I}{I_0} = \frac{(n - 1)^2 + n^2K^2}{(n + 1)^2 + n^2K^2} \tag{2}$$

where n is the refractive index, and K is the absorption index, defined through Lambert's law,

$$I = I_0 \exp\left[-4\pi Kd/\lambda_0\right] \tag{3}$$

The λ_0 denotes the wavelength of the radiation in vacuum and d is the layer thickness.

With some algebraic manipulation, equation 1 can be rewritten into the more familiar form,

$$(1 - R_\infty)^2/2R_\infty = k/s \tag{4}$$

The LHS of the equation is commonly called the *remission function* or the *Kubelka–Munk function* and is frequently denoted by $f(R_\infty)$. Experimentally, one seldom measures the absolute diffuse reflecting power of a sample, but rather the relative reflecting power of the sample compared to a suitable white standard. In that case, $k = 0$ in the spectral region of interest, $R_{\infty std} = 1$ [from equation 4], and one determines the ratio

$$R_\infty \text{ sample}/R_\infty \text{ std} = r_\infty \tag{5}$$

from which one can determine the ratio, k/s, from the remission function

$$f(r_\infty) = (1 - r_\infty)^2/2r_\infty = k/s \tag{6}$$

Taking the logarithm of the remission function gives

$$\log f(r_\infty) = \log k - \log s \tag{7}$$

Thus, if $\log f(r_\infty)$ is plotted against the wavelength or wavenumber for a sample, the curve should correspond to the absorption spectrum of the compound (as determined by transmission measurements) except for the displacement by $-\log s$ in the ordinate direction. The curves obtained by such reflectance measurements are generally called *characteristic colour curves* or *typical colour curves*. Sometimes there is a small systematic deviation in the shorter wavelength regions due to the slight increase in the scattering coefficient.

By use of modern double-beam spectrophotometers equipped with some type of a reflectance attachment, r_∞ is automatically plotted against the wavelength. Many investors replot the data as *percentage reflectance* (%R), or by use of a remission function table[4], plot $f(r_\infty)$ or k/s as a function of wavelength or wavenumber. The most common method is probably the former above.

The above brief introduction to reflectance spectroscopy outlines the most elementary principles of the technique. As would be expected, the technique is widely used for the study of solid or powdered solid samples although it can be used for liquids or paste-like materials as well. The technique is a rapid one for the determination of the 'colour' of a sample and is generally convenient to use due to readily available commercial instrumentation. Since only the surface of the sample is responsible for the reflection and absorption of the incident radiation, it is widely used in the study of the chemistry and physics of surfaces[5].

HIGH TEMPERATURE REFLECTANCE SPECTROSCOPY

Practically all of the studies in reflectance spectroscopy (it should be noted that the term reflectance spectroscopy used here will denote diffuse reflectance spectroscopy only) have been carried out at ambient temperatures or, in some cases, at sub-ambient temperatures. The latter would most probably be used in single crystal studies for the elucidation of 'hot-bands', i.e. transitions which originate from vibrationally excited ground states. However, in many cases, a great amount of additional information on a chemical system can be obtained if the reflectance spectrum of a compound is obtained at *elevated* temperatures. Normally, temperatures in the range from 100° to

P.A.C.—25/4—G

300°C have been used although there is no reason why higher temperatures could not be employed.

Two modes of investigation are used for high-temperature reflectance studies. The first is the measurement of the sample spectra at various fixed or isothermal temperatures; the second is the measurement of the change in reflectance of the sample as a function of the increasing temperature.

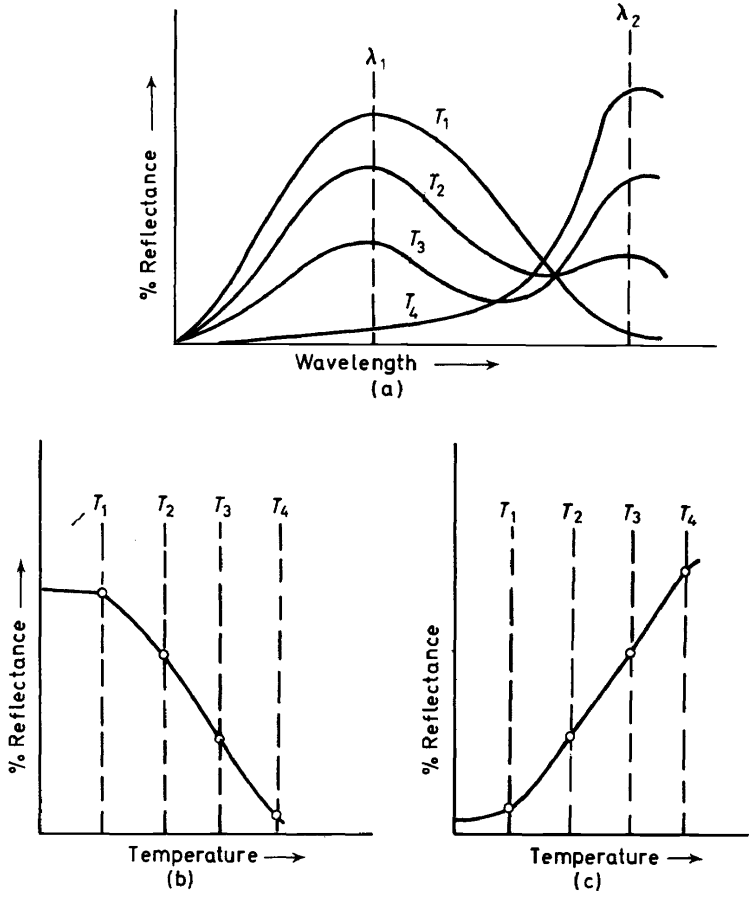

Figure 2. (a) High temperature reflectance spectra curves; (b) and (c) Dynamic reflectance spectra curves, at λ_1 and λ_2, respectively[1].

The first procedure will be called the static method or *high-temperature reflectance spectroscopy*[6] (HTRS); the second is a dynamic method and has been termed *dynamic reflectance spectroscopy*[7,8] (DRS). The two methods are illustrated in *Figure 2.* In (a), the HTRS curves, the spectra of the sample is recorded at increasing fixed temperatures, T_1 to T_4. As can be seen, the curve maximum at wavelength λ_1 decreases with increasing temperature while a new curve maximum is formed at λ_2. By measuring the spectra at small temperature increments, the minimum temperature at which the

sample begins to undergo a thermal transition can be determined. By use of the dynamic technique, these transition temperatures can be determined in a more precise manner, as shown in (b) and (c). Plotting reflectance of the sample versus temperature (b) as the sample temperature is increased at a slow fixed rate, at fixed wavelength λ_1 the reflectance is seen to decrease with an increase in temperature. Using fixed wavelength λ_2, the DRS curve in (c) is obtained which shows the increase in reflectance of the sample with increasing temperature. These *isolambdic* curves reveal the temperatures at which sample thermal transitions begin and end, and also permit the investigation of only a single thermal transition; weight loss and enthalpic effects do not interfere with the measurements. The DRS technique is useful for determining the thermal stability of a substance and also sample structural changes which are a function of temperature. Indeed, the technique shows great promise as a complementary method for other thermal techniques such as thermogravimetry, differential thermal analysis, high-temperature x-ray diffraction and others.

INSTRUMENTATION

The use of a heated sample holder to contain the compound under investigation has been described by several investigators. Asmussen and Anderson[9] studied the reflectance spectra of several $M_2[HgI_4]$ complexes at various elevated temperatures in order to investigate their thermochromic $\beta \rightarrow \alpha$ form transitions. The heated sample container consisted of a nickel-plated brass block, 60 mm in diameter by 85 mm in height, the lower end of which contained a chamber in which a small light bulb was mounted. Regulation of the current through the bulb filament permitted temperature regulation of the block. The upper end of the block contained the sample chamber which had the dimensions, 35 mm in diameter by 0.5 mm deep. A copper–Constantan thermocouple, embedded in the powdered sample, was used to detect the sample's temperature.

Kortum[2] measured the reflectance spectrum of mercury(II) iodide at 140° but did not describe the heated sample block or other experimental details. Another heated block assembly was described by Hatfield *et al.*[10]. It consisted of a metal block into which a heating element was embedded. No other details are available, such as temperature detection, sample thickness, etc.

In 1963, Wendlandt *et al.*[11] described the first of their heated sample holders for high temperature reflectance spectroscopy. The main body of the sample container was 60 mm in diameter by 11 mm thick and was machined from aluminium. The sample itself was contained in a circular indentation, 25 mm in diameter by 1 mm deep, machined on the external face of the cell. Two circular ridges were cut at regular intervals on the indentation to increase the surface area of the holder and to prevent the compacted powdered sample from falling out of the holder when it was in a vertical position. The sample holder was heated by coils of Nichrome wire wound spirally on an asbestos board and then covered with a thin layer of asbestos paper. Enough wire to provide about 15 ohms of resistance was used. The temperature of the sample was detected by a Chromel–Alumel

thermocouple contained in a two-holed ceramic insulator tube. The thermocouple junction made contact with the aluminium block directly behind the sample indentation. To prevent heat transfer from the sample holder to the integrated sphere, a thermal spacer was constructed from a loop of 0.25 in. aluminium tubing and wet shredded asbestos. After drying, the thermal spacer was cemented to the sphere and the sample holder attached to it by a spring-loaded metal clip.

A modification of the above sample holder was described by Wendlandt and George[12] and by Wendlandt[13]. The circular aluminium disc of the holder was heated by means of a cartridge heater element inserted directly behind the sample well. Two Chromel–Alumel thermocouples were placed in the block, one adjacent to the heater, the other in the bottom of the sample well so as to be in intimate contact with the compacted sample. The block thermocouple was used to control the temperature programmer while the sample thermocouple was used to detect the sample temperature.

Still another heated sample holder was described by Wendlandt and Hecht[1]. It consisted of a block of aluminium, 50 mm in diameter by 25 mm thick, into which was machined a 25 mm by 1 mm deep sample well. A 35 W stainless-steel sheathed heated cartridge embedded in the main block of the holder was used as the heater. The same two thermocouple systems, one for the temperature programmer, the other for sample temperature, were employed. For samples which evolved gaseous products, a Pyrex or quartz cover glass was used to prevent contamination of the integrating sphere.

A heated sample holder, based upon the design of Frei and Frodyma[14], which could be used for studying small samples, was recently described by Wendlandt[15]. The sample is placed as a thin layer on glass fibre cloth which is secured to the heated aluminium metal block by a metal clamp and cover glass. Dimensions of the aluminium block are 4.0 cm by 5.0 cm. The block is heated by a circular heater element contained within the holder. Electrical connections to the heater and to the thermocouple are made by means of the terminal strip mounted at the top of the assembly. Both the aluminium block and terminal strip are mounted on a 5.0 cm by 5.0 cm transite block.

Generally, in the previously described heated sample holders, few attempts were made to control the atmosphere surrounding the sample as it was heated. A cover plate of Pyrex glass or quartz was employed but its main purpose was to prevent the sample from accidentally falling into the integrating sphere of the spectroreflectometer. In order to control the sample atmosphere, the sample holder shown in *Figure 3* was constructed by Wendlandt and Dosch[16].

The sample is contained in a 1 mm by 10 mm in diameter indentation machined in the surface of a silver heater block. The circular block is 25 mm in diameter and it is heated by two 2.6 Ω Nichrome wire heaters. It is contained in an enclosure, 55 mm square and 13 mm thick. The heater is thermally insulated from the main body of the sample holder by a thin layer of ceramic fibre insulation. The sample side of the holder is enclosed by a quartz plate, 50 mm on an edge by 2 mm thick, which is held firmly in place by two metal strips. Each metal strip is fastened to the holder by two thumb screws; they can easily be removed and hence the cover plate, to facilitate sample loading and removal. A gastight seal between the cover plate and the sample holder

is provided by a 44 mm i.d. O ring. Two 0.125 in. diameter aluminium tubes, located at the top of the holder, are used to control the gas inlet and outlet to the sample chamber.

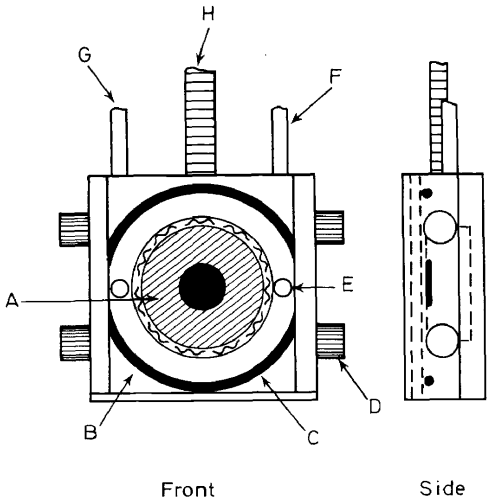

Figure 3. Schematic illustration of the heated sample holder[16]: (A) silver sample block and heater, (B) glass or quartz cover plate, (C) O ring, (D) thumb screw (one of four), (E) gas inlet to sample chamber, (F) gas outlet tube, (G) gas inlet tube, (H) connecting cable.

With the controlled atmosphere heated sample holder, it was a simple matter to connect a thermistor type thermal conductivity cell to the system and by means of an external multi-channel recorder, record the DRS and the gas evolution detection (GED) curves simultaneously.[17] This modification of the apparatus is shown in *Figure 4*. The cell was connected to a Carle Model 1000 Micro-Detector system by means of metal and rubber tubing. The thermal conductivity cell was enclosed by an aluminium block which was heated to 100°C by means of a cartridge heater. The block was

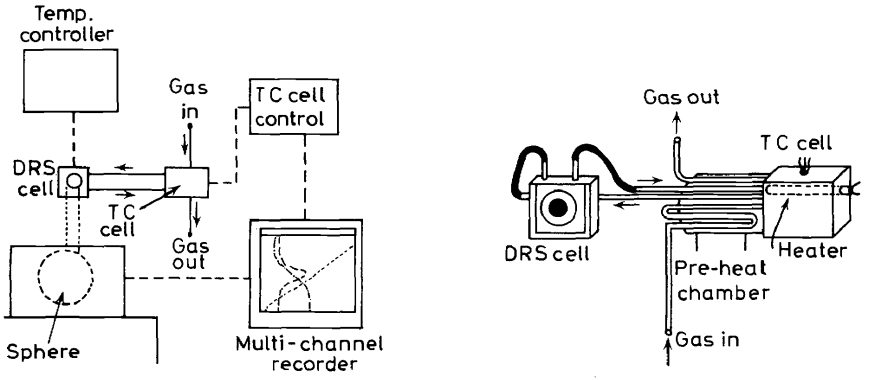

Figure 4. Schematic diagrams of DRS–GED system[17].

connected to a pre-heat chamber, also operated at 100°C, which was used to pre-heat the helium gas stream before it entered the detector. The output from the detector bridge was led into one channel of a four channel, 0–5 mV, Leeds and Northrup multi-point strip-chart potentiometric recorder. The temperature programmer from a Deltatherm III DTA instrument was used to control the temperature rise of the DRS cell. Output from the Beckman Model DK-2A spectroreflectometer was also led into the multi-channel recorder as well as the output from a thermocouple located in the DRS heater block.

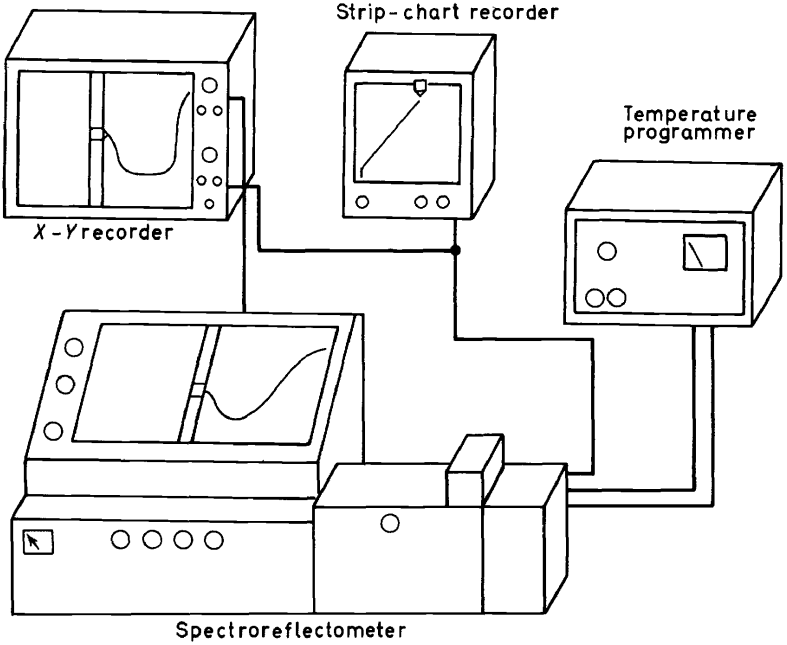

Figure 5. Schematic diagram of the HTRS–DRS system[1].

The complete HTRS–DRS system is illustrated in *Figure 5*. The high temperature sample holder is used in conjunction with a temperature programmer and two recorders. One recorder recorded the sample temperature versus time; the other, an *X/Y* recorder, was used to record reflectance versus temperature, as required for the DRS studies. A Beckman Model DK-2A or a Bausch and Lomb Spectronic 505 spectroreflectometer was employed for the spectral measurements.

APPLICATIONS OF HTRS AND DRS TO INORGANIC COMPOUNDS

1. The octahedral → tetrahedral transition in $Co(py)_2Cl_2$

The *octahedral* → *tetrahedral* structure transition of bis(pyridine)cobalt(II) chloride, $Co(py)_2Cl_2$, has been the subject of a number of investigations[9–25].

Wendlandt and George[22] studied the transition using the techniques of high temperature reflectance spectroscopy (HTRS) and dynamic reflectance spectroscopy (DRS). The thermal transition was found to begin at about 100° and was completed at about 135°. The colour change reported for the transition was from violet (*octahedral*) to a dark blue (*tetrahedral*) colour; it was stated that the change was non-reversible on cooling to room temperature.

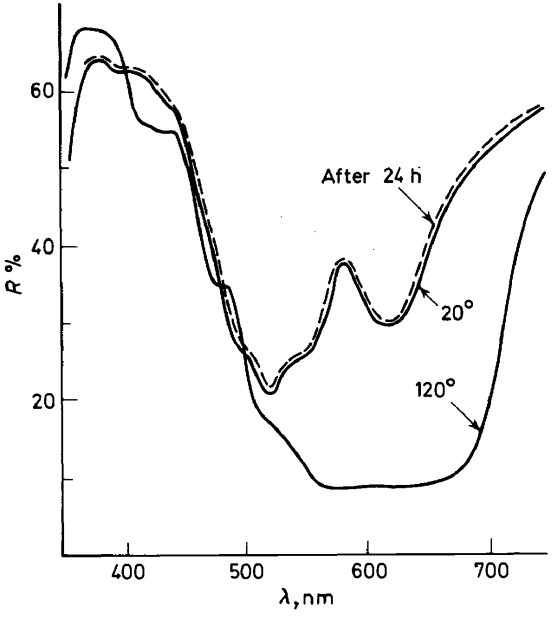

Figure 6. HTRS curves of $Co(py)_2Cl_2$ at various temperatures[18].

Recently, Wendlandt[18] reported that the structural change was actually reversible. The blue form, after standing at room temperature for 24 h, reverted back to the original violet compound. The HTRS curves of $Co(py)_2Cl_2$ at 20° and 120°C, are given in *Figure 6*. At 20°C, reflectance minima were observed in the curve at 520 and 620 nm, with shoulders at 500 and 550 nm, respectively. The compound reflected rather strongly in the 350–450 nm region and at 580 nm. The blue *tetrahedral* form, at 120°, absorbed very strongly in the 500 to 700 nm region with shoulders at 425, 480 and 510 nm, respectively. After standing 24 h at room temperature, the reflectance curve of the blue form was again recorded at 20°. As can be seen, the curve obtained was almost identical with that of the original violet compound having the *octahedral* structure. Thus it is seen that the *tetrahedral* → *octahedral* transition takes place rather slowly on standing; it does not revert back to the *octahedral* form immediately upon cooling to room temperature.

The effect of heating rate on the *octahedral* → *tetrahedral* transition is shown by the DRS curves in *Figure 7*. The heating rate varied from

1.25 deg. C/min to 10 deg. C/min, the latter value is considered to be rather high for DRS studies. Surprisingly, the procedural transition temperature was greatest (107°) for the 1.25 deg. C/min rate and lowest (95°) for the highest rate studied. However, on increasing the heating rate, the reaction temperature interval increased, from 95°–145° for the 10 deg. C/min rate to 107°–123° for the slowest heating rate. This is just the opposite to that observed in dissociation reactions involving volatile products.

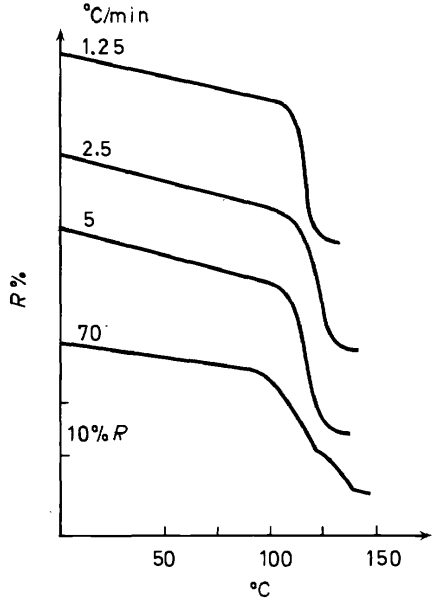

Figure 7. DRS curves of $Co(py)_2Cl_2$ at various heating rates; curves recorded at 675 nm[18].

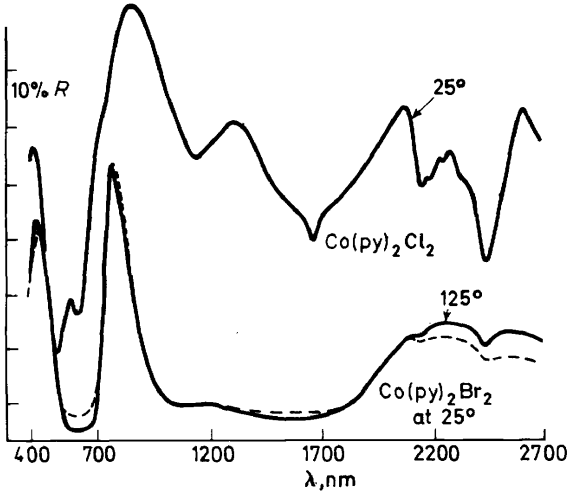

Figure 8. HRTS curves of α-$Co(py)_2Cl_2$ in the visible and near-infra-red wavelength region[15].

The spectra of $Co(py)_2Cl_2$ in the visible and near infra-red regions[15] are shown in *Figure 8*. At room temperature, reflectance minima were found at 1 140, 1670, 2 150 and 2 440 nm, respectively, for the α-form. On heating to 125°, all of these minima disappear except for a small minimum at 2440 nm. The β-form curve is practically identical to the curve obtained for *tetrahedral*-$Co(py)_2Br_2$.

2. $[Cu(en)(H_2O)_2]SO_4$

The deaquation of $[Cu(en)(H_2O)_2]SO_4$ was studied using HTRS and DRS by Wendlandt[15]. This reaction, which takes place between 75° and 150°C, follows the equation

$$[Cu(en)(H_2O)_2]SO_4(s) \rightarrow Cu(en)SO_4(s) + 2H_2O(g)$$

The HTRS curves, from 25° to 180°C, are shown in *Figure 9*. Two sets of curves are shown, one set at 25° and 75°, and the other at 150° and 180°. The first set has a peak minimum at about 625 nm (corresponding to maximum absorption) and corresponds to the curves for the initial compound while the second set has a peak minimum at 575 nm and corresponds to the curves for the deaquated compound, $Cu(en)SO_4$. Thus, the deaquation reaction must have occurred between 75° and 150°.

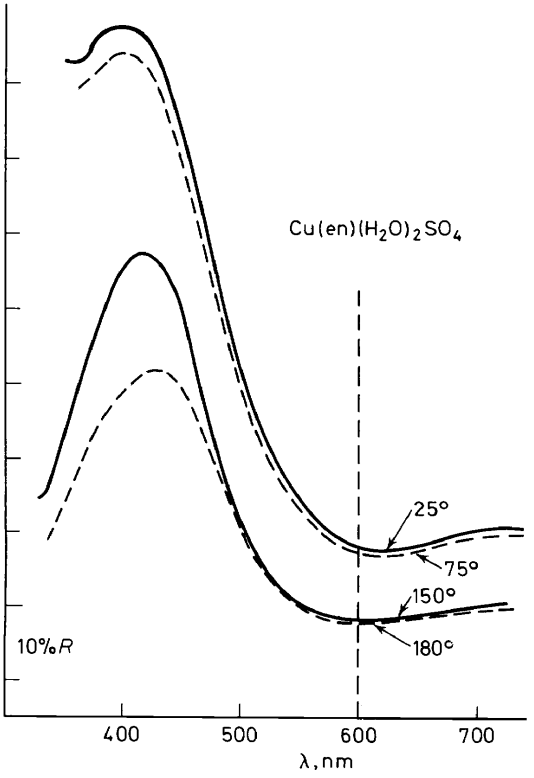

Figure 9. HTRS curves[15] of $[Cu(en)(H_2O)_2]SO_4$.

To obtain the transition temperature for the deaquation reaction, the DRS technique was employed, as shown in *Figure 10*. The transition temperature dependence upon the sample heating rate is readily seen; it varied from 115° at 6.7 deg.C/min to 165° at 45.8 deg.C/min. This behaviour is not unexpected because it occurs with practically all of the other thermal techniques where some physical property of the sample is measured as a dynamic function of temperature[13]. In all DRS studies, the sample heating rate must obviously be specified.

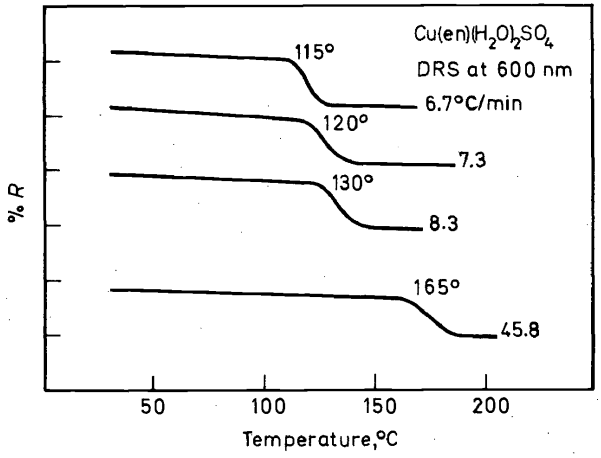

Figure 10. DRS curves of $[Cu(en)(H_2O)_2]SO_4$ at 600 nm[15].

Since the Beckman DK-2A spectroreflectometer is capable of recording the sample in the near infra-red wavelength region, the HTRS curves were recorded to 2700 nm, as shown in *Figure 11*. At room temperature, the reflectance curve contained minima (absorption bands) at 1560, 1725, 2050,

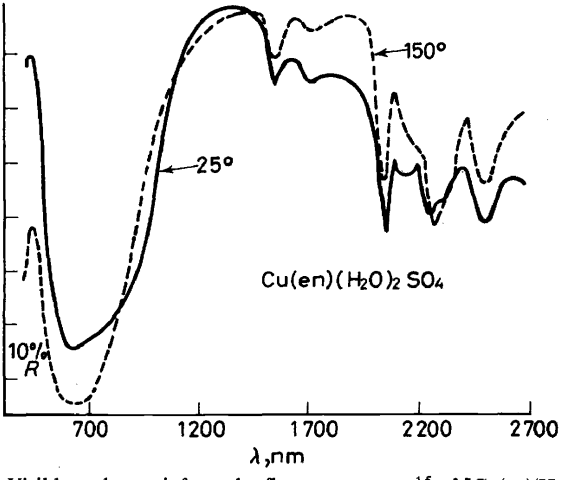

Figure 11. Visible and near-infra-red reflectance spectra[15] of $[Cu(en)(H_2O)_2]SO_4$.

2 150, 2 260 and 2 500 nm, respectively. On heating the sample to 150°, the bands at 1 560, 1 725 and 2 050 nm remained unchanged while that at 2 150 nm disappeared. The 2260 nm band shifted to 2280 nm and the 2510 nm band shifted to 2525 nm. There were rather pronounced changes in intensity for all of the bands discussed which may be due to the sample particle size changes.

3. $CuSO_4 \cdot 5H_2O$

The HTRS curves in the visible and near infra-red regions are given in *Figures 12* and *13*, while the DRS curve, at 625 nm, is given in *Figure 14*.

As in the case of $[Cu(en)(H_2O)_2]SO_4$, two sets of curves are shown for $CuSO_4 \cdot 5H_2O$ in *Figure 12*. At room temperature, the reflectance minimum occurs at about 680 nm; on heating to 135°, the minimum shifts to 715 nm.

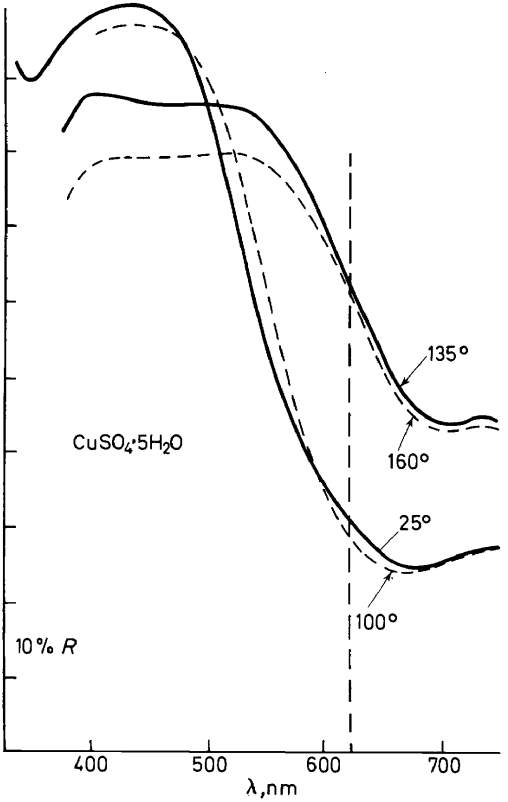

Figure 12. HTRS curves of $CuSO_4 \cdot 5H_2O$ in the visible wavelength region[15].

In this temperature range, the compositional change of the compound is that due to deaquation from $CuSO_4 \cdot 5H_2O$ to $CuSO_4 \cdot H_2O$. At still higher temperatures, i.e. 250°C, the last mole of water per mole of copper sulphate is evolved to give the anhydrous salt. In the near infra-red region at room temperature, reflectance minima were observed at 1510, 1675 and 2000 nm,

respectively. At 150°, the first two bands had disappeared while the 2000 nm had shifted to 2060 nm. A new band, at 2400 nm, was observed at the higher temperature. At still higher temperatures, 200°, all of the bands in this region were absent.

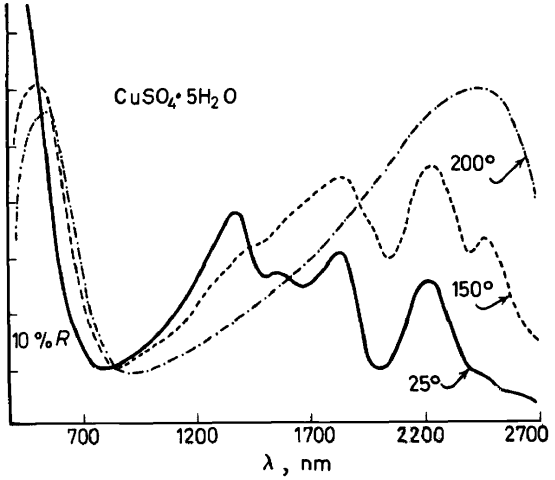

Figure 13. HTRS curves of $CuSO_4 \cdot 5H_2O$ in the visible and near-infra-red wavelength region[15].

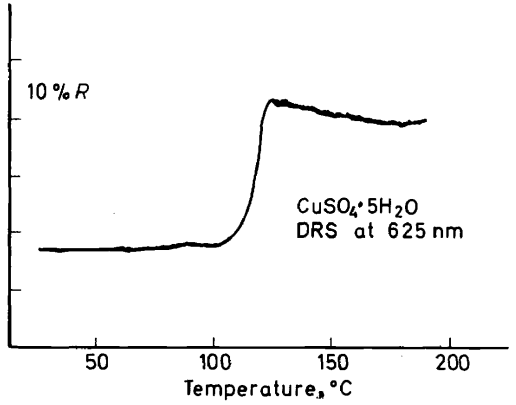

Figure 14. DRS curve[15] of $CuSO_4 \cdot 5H_2O$ at 625 nm and a heating rate of 6.7 deg. C/min.

The DRS curve, *Figure 14*, showed that a major increase in sample reflectance began at about 105° although the reflectance was gradually increased from room temperature up to 100° (about 0.1 a % R unit). About 125°, the reflectance of the compound again decreased gradually until a maximum temperature of about 200° was attained.

4. $CoCl_2 \cdot 6H_2O$

In an earlier investigation, Wendlandt and Cathers[26] studied the HTRS and DRS of the reaction between $CoCl_2 \cdot 6H_2O$ and KCl. The DRS curve

revealed that the following structural and compositional changes occurred: *octahedral*—$CoCl_2 \cdot 6H_2O$ → *tetrahedral*—$CoCl_4^{2-}$ → *octahedral*—$CoCl_2 \cdot 2H_2O$ → *tetrahedral*—$CoCl_4^{2-}$. The above reactions took place, of course, in the presence of an excess of chloride ion, hence, the final product was K_2CoCl_4 rather than anhydrous cobalt(II) chloride.

More recently, the deaquation of $CoCl_2 \cdot 6H_2O$ was investigated in the absence of potassium chloride. This compound is a rather difficult one to study because it fuses at about 50° and since the heated sample holder is mounted in a vertical position on the spectroreflectometer, the liquid $CoCl_2 \cdot 6H_2O$ cannot be retained on the sample holder. This problem was solved, however, by placing a thin layer of the powdered sample on a 25 mm diameter round cover glass which was then retained on the glass fibre cloth by the rectangular cover glass. The viscous nature of the melt prevented the compound from leaving the sample area.

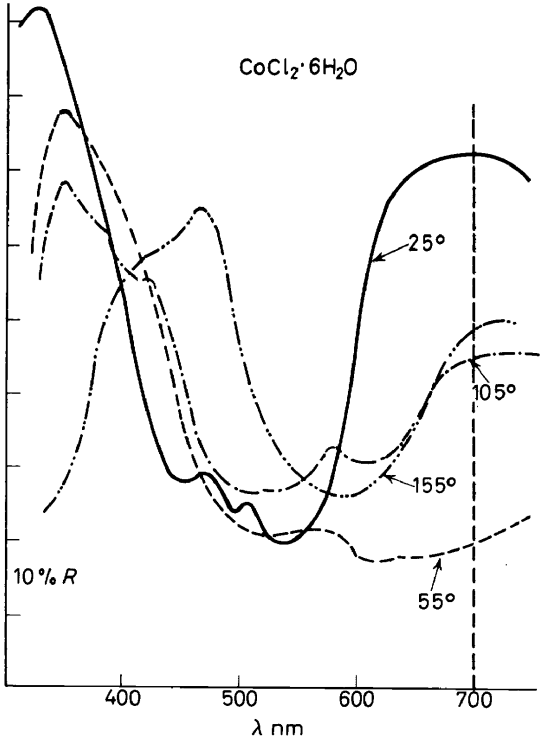

Figure 15. HTRS curves[15] of $CoCl_2 \cdot 6H_2O$.

The HTRS and DRS curves of $CoCl_2 \cdot 6H_2O$ are shown in *Figures 15* and *16*, respectively. The HTRS curves reveal a rather interesting series of structural changes, both in the liquid and solid states. At 25°, solid $CoCl_2 \cdot 6H_2O$ has an *octahedral* structure with a reflectance minimum at 535 nm and shoulder minima at 460 and 500 nm, respectively. On heating

the compound to 55°, it fused and gave a reflectance curve which had one minimum at 525 mμ and a rather broad minimum between 600 and 700 nm. This latter curve is similar to the one previously observed for a mixture of *octahedral-* and *tetrahedral*-cobalt(II) complexes by Simmons and Wendlandt[27]. Thus, a possible interpretation would be that the 55° curve is probably a mixture of *octahedral*—$CoCl_2 \cdot 6H_2O$ and *tetrahedral*—$Co[CoCl_4]$. On further heating, the mixture undergoes further deaquation and gave, at 155°, anhydrous *octahedral*—$CoCl_2$. This latter curve contained a peak minimum at 590 mμ with a shoulder minimum at 535 mμ.

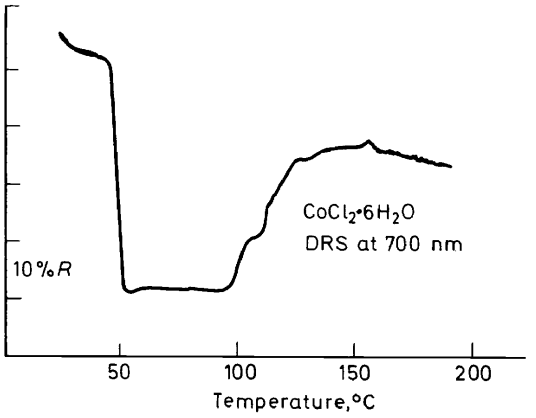

Figure 16. DRS curve[15] of $CoCl_2 \cdot 6H_2O$ at 700 nm and a heating rate of 6.7 deg. C/min.

The DRS curve, *Figure 16*, showed a pronounced decrease in reflectance at 45° which was due to the formation of the *octahedral–tetrahedral* mixture. At 100°, the reflectance of the mixture began to increase, reaching a maximum value at about 150°, then decreasing slightly above this temperature. The curve reflects the various structural changes that have been discussed previously.

5. $Ni(py)_4Cl_2$

Yang[28] studied the HTRS of the deamination of $Ni(py)_4Cl_2$, the curves of which are illustrated in *Figure 17*. The spectrum at 25°C is that for the initial compound, $Ni(py)_4Cl_2$. From 125° to 175°C, two moles of pyridine per mole of complex are lost so that the spectrum at 175°C is that for the complex, $Ni(py)_2Cl_2$. From 175° to 275°C, another pyridine is evolved so that the 275°C spectrum is that for $Ni(py)Cl_2$. The loss of pyridine and the changes in the reflectance of the initial complex are shown in the 450 nm DRS curve in *Figure 17*. The transition, $Ni(py)_4Cl_2 \rightarrow Ni(py)_2Cl_2$, began at 145° and was completed at 160°C; the loss of an additional pyridine began at 210°C and was completed at 220°C. The increase in slope throughout the DRS curve was due to the increasing sample temperature.

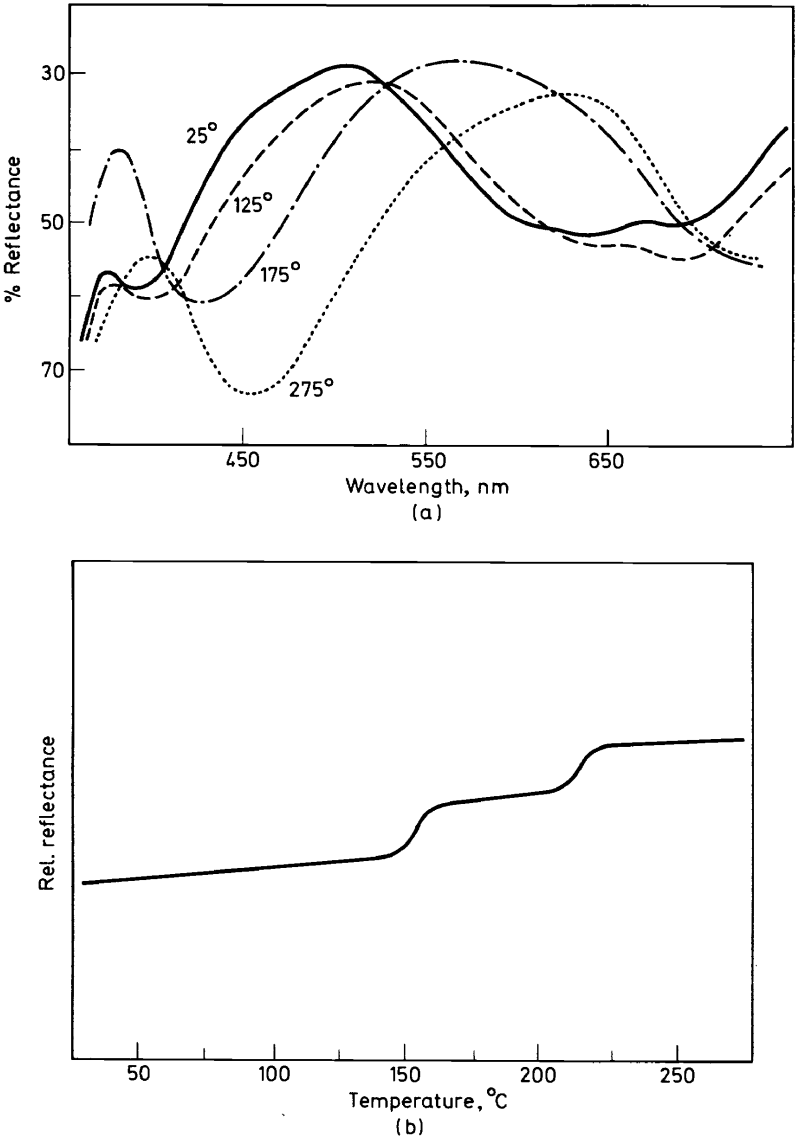

Figure 17. (a) HTRS of $Ni(py)_4Cl_2$ in an Al_2O_3 (50%) matrix; (b) DRS curve of $Ni(py)_4Cl_2$ in an Al_2O_3 (50%) matrix recorded at 450 nm[28].

6. Thermochromism of $Ag_2[HgI_4]$

The thermochromism of $Ag_2[HgI_4]$ has been of great interest since its first preparation by Caventou and Willm[29] in 1870. The transition was first investigated in a thorough manner by Ketelaar using specific heat, x-ray and electrical conductivity techniques[30–33]. Additional information concerning the colour changes[34, 36, 9], dilatometry[35], crystal structure[37, 38],

magnetic susceptibility[9], electrical conductivity[39, 40], and thermal stability[41], of the compound has been reported. The compound has been proposed as a temperature indicator[36, 42] and as a pigment for temperature indicator paints[42–44].

The thermochromism of $Ag_2[HgI_4]$ is due to an order–disorder transition which involves no less than three phases. According to Ketelaar[33], both the yellow low temperature β-modification and the red high temperature α-form contain iodide ions which are cubic close-packed while the silver and mercury ions occupy some of the tetrahedral holes. The β-form has tetragonal symmetry with the mercury ion situated at the corners of a cubic unit cell and the silver ions at the mid-points of the vertical faces. As the temperature is increased it becomes possible for the silver and mercury ions to occupy each other's lattice sites and also the two extra lattice sites (top and bottom face centres of the unit cube) which were unoccupied at lower temperatures. Above 52°C, the mercury and silver ions are completely disordered. The α-modification has, therefore, averaged face centred cubic symmetry. More recently, magnetic[39] and dielectric polarization[37, 39] measurements confirm the presence of a third phase, the β′-modification. With an increase in temperature, the silver ions become disordered occupying at random two

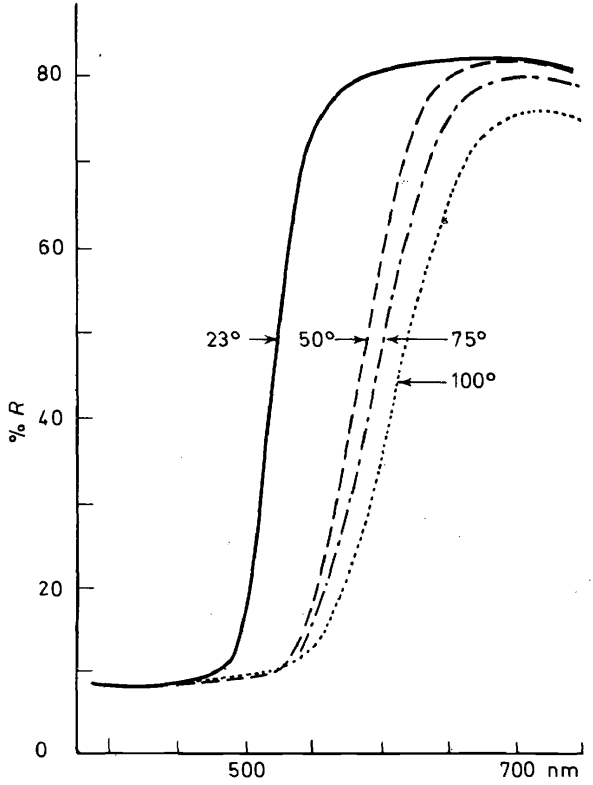

Figure 18. HTRS curves[45] of $Ag_2[HgI_4]$.

thirds of the face-centred positions of the unit cube during the $\beta \rightarrow \beta'$ transition. During the $\beta' \rightarrow \alpha$ transition, the silver and mercury ions become further disordered at random threequarters of the corners plus face centres of the unit cell. The initially obtained β' crystalline phase has a tetragonal unit cell[37] corresponding to two cubic (but not isotropic) cells stacked one on top of the other. The Patterson function suggests that some of the silver atoms are disordered, having left sites surrounded tetrahedrally by iodide ions and appearing in interstitial (octahedrally occupied) sites. The interstitial silver ions would be expected to be rather labile, since the octahedral holes are large compared to those at the tetrahedral sites. This is also apparent from the low activation energy obtained[37] for the conduction process in β-$Ag_2[HgI_4]$, 12 kcal/mole below 20°C.

The reflectance curves for $Ag_2[HgI_4]$ from 23°–100°C are shown in *Figure 18*. The yellow β-form reflects rather strongly above 500 nm with the maximum shifting to higher wavelengths during the transition to the red α-form. The change in colour is dependent upon the rate of heating. At 2.5 deg.C/min the transition is completed at a somewhat lower temperature than at the 10 deg.C/min heating rate. This heating rate is extremely rapid compared to the temperature rise of 5 deg.C/day used by Neubert and Nichols[39] in their magnetic studies. The transition temperature found here was not very well defined in that the colour change appeared to take place over the temperature range from 30° to about 60°C. Reported transition temperatures include 50.7 ± 0.2, 51.2°, 51°, 50.5° and 52°C.

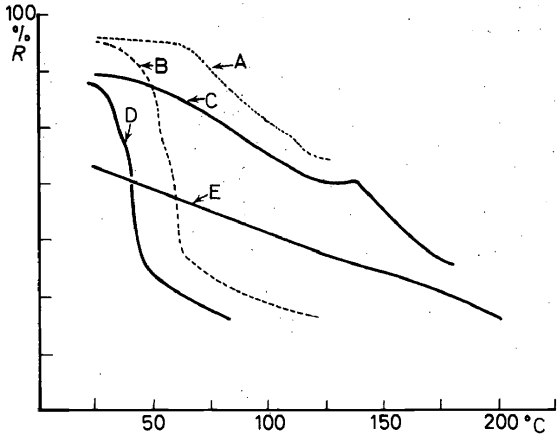

Figure 19. DRS curves of complexes (5 deg. C/min): (A) $Pb[HgI_4]$, 585 nm; (B) $Cu_2[HgI_4]$, 650 nm; (C) $Hg[HgI_4]$, 600 nm; (D) $Ag_2[HgI_4]$, 575 nm; (E) $Tl_2[HgI_4]$, 550 nm[45]

The DRS curves of a number of $M_n[HgI_4]$ complexes (M = Pb, Cu, Hg, Ag and Tl) are given in *Figure 19*. All of the compounds exhibit a rather sharp thermochromic transition with the exception of $Tl_2[HgI_4]$. The latter compound is reported[9] to have a transition at 116.5°C; however, it is not evident from the DRS curve. The change in reflectance of the compound appears to decrease linearly with temperature.

HIGH TEMPERATURE SCANNING MICROREFLECTANCE SPECTROSCOPY AND DYNAMIC MICROREFLECTANCE SPECTROSCOPY

The use of high temperature reflectance and dynamic reflectance spectroscopy has generally been limited to macro-samples, 0.10–0.50 g. Smaller samples can be investigated if microscopic techniques are employed such as combining reflectance spectroscopy with a low power (100 ×) microscope. Such an apparatus has been described by Wendlandt, as shown in *Figure 20*.

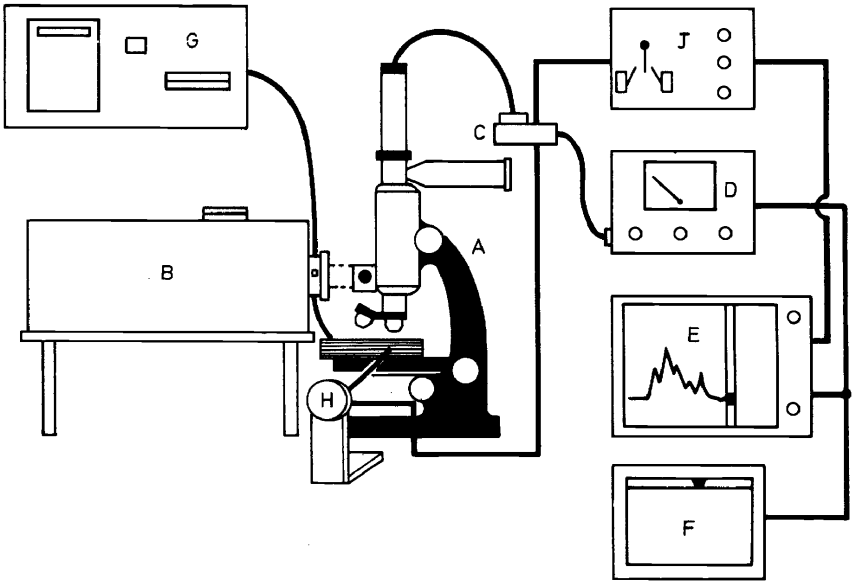

Figure 20. Microreflectance apparatus; A, B&L microscope; B, B&L monochromator and lamp; C, photomultiplier tube; D, amplifier and power supply; E, X/Y recorder; F, strip-chart recorder; G, Mettler hot-stage; H, reversible motor; J, relay and timer.

The apparatus consists of a low power (100 × generally) reflection type microscope, A, which is illuminated by means of a monochromator, B. The reflected radiation is detected by a photomultiplier tube, C, and amplifier, D, and recorded on an X/Y recorder, E, or a strip chart recorder, F. In order to heat the sample to 250°C, a Mettler Model FP-2 hot-stage, G, is employed. Either isothermal ($\pm$ 1 deg.C) or dynamic sample temperatures may be attained by this device. The sample is moved through the illuminated optical field by means of the reversible motor, H. The motor is reversed at preset intervals by a relay circuit and timer, J. Thus, it is possible to scan the reflectance from the sample which may consist of a single crystal or a powdered mixture. Powdered samples may be placed directly on the heated microscope slide or else placed in 0.9–1.1 mm i.d. glass capillary tubes. In the latter case, it is possible to obtain the reflectance curve of a sample contained in a sealed tube.

Two modes of operation of the apparatus are possible: (a) the scanning mode in which the sample surface reflectance is recorded as a function of scanning distance at ambient room temperature or at elevated temperatures; and (b) the change in reflectance of the sample as a function of temperature. The former mode is called high temperature scanning microreflectance (SMR), while the latter is called dynamic microreflectance (DMR). The use of these two modes is illustrated by the deaquation of $CuSO_4 \cdot 5H_2O$.

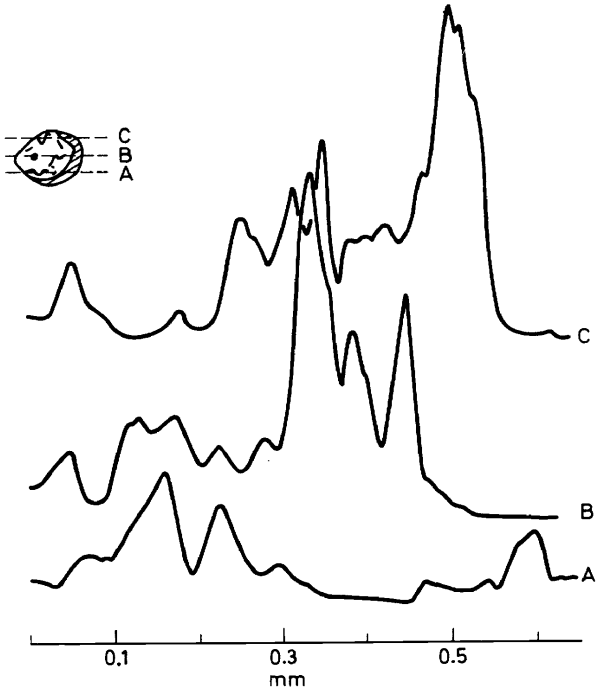

Figure 21. Scanning microreflectance curves of a single crystal of $CuSO_4 \cdot 5H_2O$ at a wavelength of 450 nm and at a temperature of 30 C (100 × magnification)[46].

The scanning microreflectance curves of a single crystal of $CuSO_4 \cdot 5H_2O$[46] at room temperature are shown in *Figure 21*. The curves represent the reflectance of the crystal surface at scans at points A, B and C. Since the reflectance geometry of 90°/90° was used, the curve maxima represent maximum specular reflectance from the crystal surface. Thus, surfaces perpendicular to the incident beam reflect the strongest, giving the curve peak maxima. The curves are not very reproducible from crystal to crystal due to the different surfaces of the individual crystals.

The SMR curves of the same crystal at various temperatures are illustrated in *Figure 22*. The curves changed little on increasing the temperature of the crystal from 30°–50°C. However, at 70°C, the specular reflectance maxima all showed a general decrease which became more pronounced as the temperature was increased from 80° to 100°C. The decrease in the specular reflectance of the crystals was due to the formation of a surface layer of

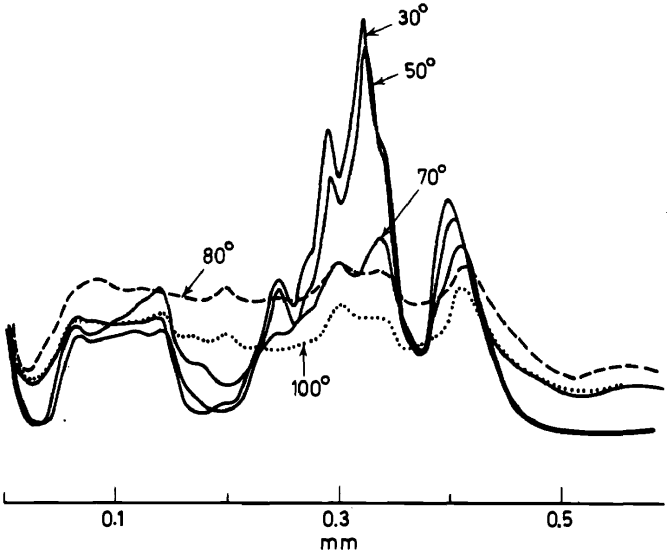

Figure 22. Scanning microreflectance curves of a single crystal of $CuSO_4 \cdot 5H_2O$ at various temperatures; wavelength of incident light 450 nm, 100 × magnification[46].

$CuSO_4 \cdot 3H_2O$ which is more opaque than the original compound. Thus, the formation of the former can easily be followed by the SMR technique.

The evolution of liquid water in the deaquation of $CuSO_4 \cdot 5H_2O$ is vividly illustrated by the microreflectance of powdered $CuSO_4 \cdot 5H_2O$ in sealed and open glass capillary tubes, as shown in *Figure 23*. In an open capillary tube, the sample reflectance decreased as the temperature increased, due to the evolution of liquid water. On further heating, the reflectance increased due to the vaporization of the water and the formation of $CuSO_4 \cdot H_2O$. In a sealed-tube, the reflectance of the samples decreased as the temperature was increased. However, since the liquid water was confined to the capillary tube, the reflectance did not increase again on further heating.

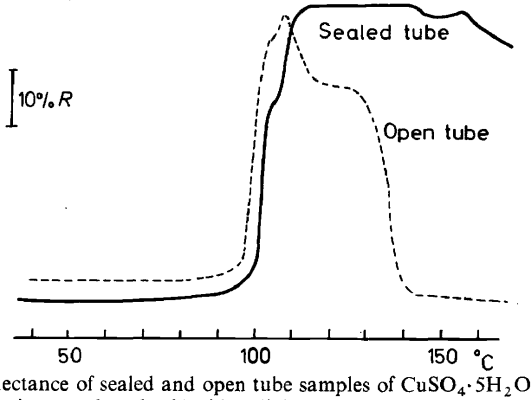

Figure 23. Microreflectance of sealed and open tube samples of $CuSO_4 \cdot 5H_2O$ heating rate of 10 deg. C/min: wavelength of incident light, 450 nm: 80 × magnification[46].

REFERENCES

[1] W. W. Wendlandt and H. G. Hecht, *Reflectance Spectroscopy*, Chapters 3 and 4. Interscience: New York (1966).
[2] G. Kortum, *Trans. Faraday Soc.* **58**, 1624 (1962).
[3] P. Kubelka and F. Munk, *Z. Techn. Phys.* **12**, 593 (1931).
[4] Ref. 1, pp 275–279.
[5] Ref. 1. Chap. 8.
[6] W. W. Wendlandt, P. H. Franke and J. P. Smith. *Analyt. Chem.* **35**, 105 (1963).
[7] W. W. Wendlandt, *Science*, **140**, 1085 (1963).
[8] Anon., *Chem. Engng News*, p 62 (15 April 1963).
[9] R. W. Asmussen and P. Anderson, *Acta Chem. Scand.*, **12**, 939 (1958).
[10] W. E. Hatfield, T. S. Piper and U. Klabunde, *Inorg. Chem.* **2**, 629 (1963).
[11] W. W. Wendlandt. P. H. Franke and J. P. Smith. *Analyt. Chem.* **35**. 105 (1963).
[12] W. W. Wendlandt and T. D. George, *Chemist-Analyst*, **53**, 100 (1964).
[13] W. W. Wendlandt, *Thermal Methods of Analysis*, Chap. 10. Interscience: New York (1964).
[14] R. W. Frei and M. M. Frodyma, *Analyt. Chim. Acta*, **32**, 501 (1965).
[15] W. W. Wendlandt, in *Modern Aspects of Reflectance Spectroscopy*, W. W. Wendlandt (Ed.). Plenum: New York (1968).
[16] W. W. Wendlandt and E. L. Dosch, *Thermochim. Acta*, **1**, 103 (1970).
[17] W. W. Wendlandt and W. S. Bradley, *Thermochim. Acta*, **1**, 143 (1970).
[18] W. W. Wendlandt, *J. Thermal Anal.* **1**, 469 (1970).
[19] E. G. Cox, A. J. Shorter, W. Wardlaw and W. J. R. Way, *J. Chem. Soc.* 1556 (1937).
[20] J. D. Dunitz, *Acta Cryst., Camb.* **10**, 307 (1957).
[21] D. P. Mellor and C. D. Coryell, *J. Amer. Chem. Soc.* **60**. 1786 (1938).
[22] W. W. Wendlandt and T. D. George, *Chemist-Analyst*, **53**, 71 (1964).
[23] L. R. Ocone, J. R. Soulen and B. P. Block, *J. Inorg. Nucl. Chem.* **15**, 76 (1960).
[24] G. Beech, C. T. Mortimer and E. G. Tyler, *J. Chem. Soc.* 925 (1967).
[25] I. G. Murgulescu, E. Segal and D. Fatu, *J. Inorg. Nucl. Chem.* **27**, 2677 (1965).
[26] W. W. Wendlandt and R. E. Cathers, *Chemist-Analyst*, **53**, 110 (1964).
[27] E. L. Simmons and W. W. Wendlandt, *J. Inorg. Nucl. Chem.* **28**, 2187 (1966).
[28] W. Y. Yang, unpublished results.
[29] E. Caventou and E. Willm, *Bull. Soc. Chim. Fr.* **13**, 194 (1870).
[30] J. A. A. Ketelaar, *Z. Kristallogr.* **87**, 436 (1934).
[31] J. A. A. Ketelaar, *Z. Phys. Chem.* **B26**, 327 (1935).
[32] J. A. A. Ketelaar, *Z. Phys. Chem.* **B30**, 35 (1938).
[33] J. A. A. Ketelaar, *Trans. Faraday Soc.* **34**, 874 (1938).
[34] L. Suchow and P. H. Keck, *J. Amer. Chem. Soc.* **75**, 518 (1953).
[35] D. G. Thomas, L. A. K. Staveley and A. F. Cullis, *J. Chem. Soc.* 1727 (1952).
[36] C. H. Bachman and J. B. Maginnis, *Amer. J. Phys.* **19**, 424 (1951).
[37] C. E. Olson and P. M. Harris, *Phys. Rev.* **86**, 651 (1952); U.S. Department of Commerce, Office Tech. Ser., PB Dept. 156, 106, 61 pp (1959).
[38] H. Hahn, G. Frank and W. Klinger, *Z. Anorg. Allgem. Chem.* **279**, 271 (1955).
[39] T. J. Neubert and G. M. Nichols, *J. Amer. Chem. Soc.* **80**, 2619 (1958).
[40] J. Rothstein, *Phys. Rev.* **98**, 271 (1955).
[41] E. A. Heintz, *J. Inorg. Nucl. Chem.* **21**, 64 (1961).
[42] W. S. Andrews. *Gen. Elect. Rev.* **29**. 521 (1926).
[43] H. G. Perez. *Quim. e Industr. Sao Paulo*, **4**. 137 (1936).
[44] Y. Horiguchi, T. Funayama and T. Nakanishi, *Sci. Pap. Inst. Phys. Chem. Res. Tokyo*, **53**, 274 (1959).
[45] W. W. Wendlandt and W. S. Bradley, *Thermochim. Acta*, **1**. 529 (1970).
[46] W. W. Wendlandt, *Thermochim. Acta*, **1**. 419 (1970).